JCTC Journal of Chemical Theory and Computation

Oscillator Strength: How Does TDDFT Compare to EOM-CCSD?

Marco Caricato,*,† Gary W. Trucks,† Michael J. Frisch,† and Kenneth B. Wiberg‡

Gaussian, Inc., 340 Quinnipiac St., Bldg. 40, Wallingford, Connecticut 06492, United States, and Department of Chemistry, Yale University, 225 Prospect St., New Haven, Connecticut 06511, United States

Received November 16, 2010

Abstract: In this work, we compare a large variety of density functionals against the equation of motion coupled cluster singles and doubles (EOM-CCSD) method for the calculation of oscillator strengths. Valence and Rydberg states are considered for a test set composed of 11 small organic molecules. In our previous work, the same systems and methods were tested against experimental results for the excitation energies. The results from this investigation confirm our previous findings, i.e., that there is a large difference between the functionals. For the oscillator strength, the average best agreement with EOM-CCSD is provided by CAM-B3LYP followed by LC-ωPBE and, to a lesser extent, B3P86 and LC-BLYP.

1. Introduction

Molecular UV/vis spectroscopy is routinely used in many areas of experimental research, and computational simulations of spectra have become an increasingly important, often essential tool for the interpretation of experiments. Nonetheless, the accurate simulation of molecular UV/vis spectra still represents a theoretically difficult challenge. Many methods and approximations have been developed to tackle this challenge. In particular, the advent of the time-dependent density functional theory (TDDFT)[1–3] within the adiabatic approximation has allowed the study of a large variety of molecules in different fields. Since the exact functional is not known, a myriad of approximate functionals has been proposed, and new ones are introduced every year. This constitutes a problem for the investigators, especially for nonspecialists, who want to take advantage of the computational efficacy of TDDFT.

Several papers have appeared in recent years that compare different functionals on different molecular systems for the calculation of vertical excitation energies.[4–16] In our previous work on this property,[12] we examined 11 small organic molecules for which extensive experimental and theoretical data in the gas phase are available:[17–29] a total of 69 states, 30 valence and 39 Rydberg in nature. Our set included a variety of density functionals: local spin density approximation (LSDA), generalized gradient approximation (GGA), GGA with kinetic energy density or meta-GGA (M-GGA), hybrid GGA (H-GGA), and hybrid meta-GGA (HM-GGA) as well as functionals that separate short- and long-range exchange contributions (with and without the correct long-range limits). Additionally, we considered four single reference wave function (WF) methods: configuration interaction with single excitations (CIS),[30] CIS with perturbative double excitations correction (CIS(D)),[31] random phase approximation (RPA),[32] and the highly accurate and computationally demanding equation of motion coupled cluster singles and doubles (EOM-CCSD).[33–35] Only single reference methods were considered because their results are unambiguous; therefore, they represent useful computational tools even for nontheoretically trained investigators. The computed data were compared to experimental results. As expected, EOM-CCSD was revealed to be the most accurate among the selected methods. This level of theory is often regarded as the best compromise between accuracy and computational cost for small- and medium-sized molecules, and it has the advantage that the quality of the wave function can be systematically improved by including more excitations in the wave operator.[33–35] On the other hand, there is not a systematic way to improve a particular functional, and its

* To whom correspondence should be addressed. E-mail: marco@gaussian.com.

† Gaussian, Inc.

‡ Yale University.

10.1021/ct100662n
Published on Web 12/22/2010

Table 1. List of Functionals Used in This Work

	year	type	% HF		year	type	% HF
LSDA[44,48]	1951	LSDA		B3VP86[45,47,48,50]	1993	H-GGA	20
BLYP[45,46]	1988	GGA		PBE1PBE[53,54,69,70]	1997	H-GGA	25
OLYP[49,46]	2001	GGA		THCTHHYB[57]	2002	HM-GGA	15
BP86[45,50]	1988	GGA		TPSSh[59,73]	2003	HM-GGA	10
BVP86[45,48,50]	1988	GGA		M05[60]	2005	HM-GGA	28
PBEPBE[53,54]	1997	GGA		BH&H,[44,46,48 a]	1993	H-GGA	50
HCTH[51,55,56]	2001	GGA		BH&HLYP,[44–46,48 a]	1993	H-GGA	50
THCTH[57]	2002	M-GGA		BMK[62]	2004	HM-GGA	42
VSXC[52]	1998	M-GGA		M05−2X[61]	2006	HM-GGA	56
TPSSTPSS[59]	2003	M-GGA		HSE1PBE[63]	2003	H-GGA	25−0[a]
O3LYP[46,49,58]	2001	H-GGA	11.61	CAM-B3LYP[64]	2004	H-GGA	19−65[b]
B3LYP[45–47,71,72]	1994	H-GGA	20	LC-BLYP[45,46,65,66]	2001	H-GGA	LC[c]
B3P86[45,47,50]	1993	H-GGA	20	LC-ωPBE[65–68]	2006	H-GGA	LC[c]

[a] Note that these are not the same as the half-and-half functionals proposed by Becke.[74] [b] Short-range−long-range. [c] The percentage of HF exchange increases as described in refs 65–68.

ability to compute a particular property must be tested against experimental results or a high ab initio level of theory. The results of our previous work[12] demonstrated that there are large differences between the functionals and that new functionals do not necessarily outperform older ones, at least for the range of transitions we studied. In fact, a relatively old functional, B3P86, performed as well as more recent ones such as CAM-B3LYP and LC-ωPBE; although the latter two were designed for the description of excited states, while the former was not.

Nevertheless, the excitation energy is only one part of a UV/vis spectrum; the other part is the intensity of the bands. This depends on the oscillator strength, which is related to the probability of the transition from the ground to an excited state when the molecule interacts with an electric field.[32] In the present literature, there are few comparisons of the performance of functionals for the calculation of this property.[7–10,36–43] In principle, the oscillator strength can be directly extracted from experimental results. Unfortunately, this is often difficult because of line broadening and overlapping of the excitation bands, and often the comparison with experimental oscillator strengths can only be qualitative. Therefore, in this work, the functionals are tested against the EOM-CCSD results. We only focus on single reference methods since their use is straightforward, as mentioned above. Although it is not expected that this level of theory is exact, EOM-CCSD is a well-defined reference[7–9] and can be systematically improved. The same states and molecules used in ref 12 are tested in the first part of the paper, and in the second part, a portion of the spectra is simulated by superimposing Gaussian line shapes in order to mimic the experimental bands (neglecting the vibronic structure, which is beyond the scope of the present work).

This paper is organized as follows. Section 2 describes the methods, the test systems, and other details of the calculations. Section 3 reports the results for the states used in ref 12, while section 4 contains the simulated spectra. An overall discussion of the results and concluding remarks are reported in section 5.

2. Computational Details

The selected methods are the same as those employed in ref 12. There are four WF methods: CIS, CIS(D), RPA, and EOM-CCSD. The approximate density functionals are listed in Table 1. The molecules we consider are also those from ref 12. There are three alkenes: ethylene (D_{2h}), isobutene (C_{2v}), and trans-1,3-butadiene (C_{2h}, we refer to this molecule simply as "butadiene" in the following); three carbonyl compounds: formaldehyde (C_{2v}), acetaldehyde (C_s), and acetone (C_{2v}); and five azabenzenes: pyridine (C_{2v}), pyrazine (D_{2h}), pyrimidine (C_{2v}), pyridazine (C_{2v}), and 1,2,4,5-tetrazine (D_{2h}, s-tetrazine). Their geometries were optimized at the MP2/6-311+G(d,p) level of theory (the geometries are available in the Supporting Information of ref 12). The vertical excitation energies and oscillator strengths are computed with the 6-311(3+,3+)G(d,p) basis set (the extra diffuse functions are available in the Supporting Information). All of the calculations are performed with a development version of the Gaussian suite of programs.[75] CIS(D) only corrects the CIS transition energy, but not the CIS transition dipole; therefore, the oscillator strengths for this method are computed as

$$f_i^{\mathrm{CIS(D)}} = \frac{2}{3}|\mu_{i0}^{\mathrm{CIS}}|^2 \Delta E_i^{\mathrm{CIS(D)}} \quad (1)$$

where f_i is the oscillator strength for the ith state, μ_{i0} is the transition dipole, and ΔE_i is the transition energy in atomic units.

The data in section 3 only refer to the states that we considered in ref 12, which have experimental data for the excitation energies. As outlined in section 1, experimental oscillator strengths are often nonquantitative; thus, the benchmark in this work is EOM-CCSD/6-311(3+,3+)G(d,p), which has shown great reliability in the study of excited states of small organic molecules.[7–9,76,77] We did not consider the transition properties computed with the linear response CCSD approach (LR-CCSD)[78,79] because it has been shown that the difference between LR- and EOM-CCSD is negligible for small molecules.[80,81] Since many states and many methods are compared, and oscillator strengths may differ by several orders of magnitude between different states, we perform a linear least-squares fit between the oscillator strengths computed with a particular method as a function of the reference (EOM-CCSD). The data reported in section 3 (X^L) are given as the slope of the line (with zero intercept)

that best fits the oscillator strengths computed with a particular method compared to EOM-CCSD:

$$f_i^{\text{method}} = X^L f_i^{\text{EOM-CCSD}} \quad (2)$$

We also report the R^2 parameter, which indicates how close the data points are to a line. This choice for the representation of the results provides the proper weight to the excited states according to the magnitude of their oscillator strengths. Indeed, many states in ref 12 have small oscillator strength or are symmetry-forbidden (they appear in the experimental spectrum because of vibrational symmetry breaking). All of the oscillator strengths are available in the Supporting Information.

Section 4 contains the simulated spectra obtained from the oscillator strengths by adding Gaussian line shapes through the Harada−Nakanishi equation:[82]

$$\varepsilon(\nu) = \frac{f_i}{3.483 \times 10^{-5}\sqrt{\pi}\sigma} \, e^{-((\nu - \nu_i)/\sigma)^2} \quad (3)$$

where ε is the extinction coefficient, ν is the excitation energy in eV, and σ is a parameter that we choose equal to 0.4 eV. We consider the region of the spectrum spanned by the first 20 states of EOM-CCSD ($\Delta E < 7-9$ eV, depending on the molecule). For the other methods, we include all the states necessary to have a complete description of the corresponding EOM-CCSD bands. Thus, the number of states considered is larger than in ref 12 and section 3. Furthermore, since including all of the methods would make the spectra unreadable, we only select 11 methods: CIS, LSDA, BLYP, B3LYP, B3P86, PBE1PBE, M05, CAM-B3LYP, LC-BLYP, LC-ωPBE, and EOM-CCSD. CIS and LSDA are the simplest among the WF and DFT methods. The other functionals are chosen among the various classes, in particular, those for which a long-range correction is available. We choose not to compare the simulated spectra with the experimental UV/vis spectra because the latter contain considerable vibronic structure, which strongly influences the shape and size of the bands. In contrast, the simple band structure provided by eq 3 would make the comparison with the experimental spectra difficult. Therefore, EOM-CCSD is the reference method also in this case.

3. Statistical Analysis

The values of X^L for alkenes, carbonyls, and azabenzenes are reported in Tables 2−4, respectively. These data are also grouped together in a graphical form in Figures 1 and 2. Figure 1 reports $X^L - 1$ for the single molecules, while Figure 2 reports $X^L - 1$ collectively for the groups of compounds (in Figure 1, the WF methods are not included because their X^L values are very large in many instances). In these figures, a negative value corresponds to a scaling factor smaller than 1, and a positive value to a factor larger than 1. The R^2 parameters are reported in Figures 3 and 4 for the single molecules and for the molecular groups, respectively (the numerical values are available in the Supporting Information). In the following discussion, we consider "good" the performance of a method that provides $0.66 < X^L < 1.5$ and $0.8 < R^2 \leq 1$. Obviously, the best performances are those where the X^L and R^2 parameters approach 1.

Table 2. X^L for the Alkenes

	ethylene	isobutene	butadiene	all
RPA	1.16	1.94	1.24	1.25
CIS	1.43	1.69	1.45	1.45
CIS(D)	1.49	1.65	1.47	1.48
LSDA	0.73	1.01	0.89	0.86
BLYP	0.53	0.21	0.77	0.69
OLYP	0.42	0.42	0.67	0.60
BP86	0.61	0.31	0.85	0.77
BVP86	0.61	0.31	0.85	0.77
PBEPBE	0.61	0.41	0.83	0.76
HCTH	0.61	0.71	0.85	0.79
THCTH	0.61	0.61	0.87	0.79
VSXC	0.72	0.13	0.90	0.83
TPSSTPSS	0.62	0.28	0.84	0.76
O3LYP	0.48	0.57	0.80	0.71
B3LYP	0.75	0.78	0.92	0.87
B3P86	0.88	1.35	0.97	0.97
B3VP86	0.79	0.81	0.95	0.91
PBE1PBE	0.81	0.93	0.96	0.92
THCTHHYB	0.72	0.78	0.93	0.87
TPSSh	0.55	0.50	0.90	0.80
M05	0.85	1.25	0.95	0.94
BH&H	0.96	1.38	1.07	1.05
BH&HLYP	0.96	1.37	1.07	1.05
BMK	0.88	1.05	1.01	0.98
M05−2X	1.00	2.11	1.06	1.09
HSE1PBE	0.83	0.99	0.96	0.93
CAM-B3LYP	0.95	1.38	1.02	1.02
LC-BLYP	1.06	2.15	1.12	1.15
LC-ωPBE	1.03	2.10	1.09	1.12

Table 3. X^L for the Carbonyls

	formaldehyde	acetaldehyde	acetone	all
RPA	3.01	1.80	3.32	2.53
CIS	2.72	1.35	5.09	2.65
CIS(D)	2.25	1.01	4.30	2.16
LSDA	0.43	0.74	0.25	0.53
BLYP	0.26	0.50	0.26	0.37
OLYP	0.43	0.62	0.26	0.48
BP86	0.23	0.43	0.26	0.33
BVP86	0.23	0.43	0.26	0.33
PBEPBE	0.24	0.55	0.26	0.38
HCTH	0.26	0.78	0.29	0.50
THCTH	0.27	0.63	0.27	0.43
VSXC	0.20	0.39	0.25	0.29
TPSSTPSS	0.21	0.46	0.25	0.33
O3LYP	0.51	0.66	0.27	0.52
B3LYP	0.51	0.66	0.27	0.52
B3P86	0.58	0.75	0.31	0.59
B3VP86	0.44	0.60	0.26	0.47
PBE1PBE	0.51	0.66	0.26	0.52
THCTHHYB	0.38	0.58	0.25	0.44
TPSSh	0.31	0.51	0.25	0.38
M05	0.67	0.86	0.30	0.67
BH&H	0.74	0.87	0.58	0.76
BH&HLYP	0.78	0.88	0.65	0.80
BMK	0.52	0.53	0.36	0.49
M05−2X	0.85	0.99	0.48	0.83
HSE1PBE	0.47	0.67	0.26	0.51
CAM-B3LYP	0.81	0.90	0.80	0.85
LC-BLYP	1.38	1.39	1.19	1.34
LC-ωPBE	0.95	1.06	0.86	0.98

In the alkene group, eleven transitions are considered for ethylene, two for isobutene, and seven for butadiene. The most intense states for these molecules are the first B_{1u} state

Table 4. X^L for the Azabenzenes

	pyridine	pyrazine	pyrimidine	pyridazine	S-tetrazine	all
RPA	2.44	1.65	1.96	2.75	1.02	1.78
CIS	2.79	2.14	2.26	2.94	1.44	2.22
CIS(D)	2.48	1.95	2.03	2.63	1.13	2.01
LSDA	1.02	0.94	1.45	0.65	0.67	0.99
BLYP	1.04	0.92	0.83	0.74	0.70	0.91
OLYP	0.83	0.70	0.52	0.77	0.67	0.69
BP86	1.02	0.98	1.14	0.92	0.71	0.99
BVP86	1.03	0.97	1.14	0.92	0.71	0.99
PBEPBE	1.03	0.95	0.56	0.77	0.67	0.90
HCTH	0.98	0.87	1.29	0.64	0.70	0.91
THCTH	1.12	0.97	1.23	0.73	0.74	1.00
VSXC	1.16	0.89	0.96	0.61	0.77	0.91
TPSSTPSS	1.05	0.74	1.11	0.93	0.73	0.81
O3LYP	1.41	1.16	1.42	1.14	0.68	1.20
B3LYP	1.39	1.17	1.30	1.21	0.74	1.20
B3P86	1.39	1.22	1.43	1.17	0.74	1.24
B3VP86	1.39	1.21	1.41	1.12	0.74	1.24
PBE1PBE	1.46	1.26	1.46	1.18	0.77	1.28
THCTHHYB	1.28	1.15	1.31	0.97	0.71	1.17
TPSSh	1.24	1.02	1.46	0.93	0.70	1.08
M05	1.67	1.39	1.69	1.19	0.66	1.42
BH&H	1.88	1.49	1.77	1.49	0.92	1.54
BH&HLYP	1.81	1.43	1.65	1.48	0.90	1.47
BMK	1.59	1.38	1.64	1.22	0.79	1.41
M05−2X	1.95	1.60	2.01	1.41	0.78	1.65
HSE1PBE	1.46	1.25	1.46	1.16	0.76	1.28
CAM-B3LYP	1.57	1.33	1.58	1.21	0.86	1.36
LC-BLYP	1.76	1.47	1.76	1.42	0.99	1.51
LC-ωPBE	1.66	1.42	1.73	1.31	0.96	1.46

for ethylene ($f^{\text{EOM-CCSD}}_{1B_{1u}} = 0.3520$), the A_1 state for isobutene ($f^{\text{EOM-CCSD}}_{A_1} = 0.1525$), and the first two B_u states for butadiene ($f^{\text{EOM-CCSD}}_{1B_u} = 0.6169$ and $f^{\text{EOM-CCSD}}_{2B_u} = 0.1636$). The oscillator strengths for the remaining states are on the order of 7×10^{-2} and lower. The WF methods overestimate the oscillator strength for this class of molecules, especially for isobutene. RPA, however, performs reasonably well for ethylene and butadiene (see Table 2). On the other hand, most of the density functionals underestimate the reference at least until a large percentage of HF exchange is introduced (see Table 2 and Figures 1 and 2). Hybrid functionals perform quite well for these molecules, although some provide a large overestimation for isobutene. This is the case for M05-2X, LC-BLYP, and LC-ωPBE, and to a lesser extent for B3P86, M05, BH&H, BH&HLYP, and CAM-B3LYP. The R^2 values are remarkably good with almost all of the methods for the individual molecules and as a group, as shown in Figures 3 and 4.

For the carbonyls, we consider eleven transitions for formaldehyde, six for acetaldehyde, and eight for acetone. The largest oscillator strengths are on the order of 7×10^{-2}. The WF methods largely overestimate the reference. CIS(D) reduces the value of X^L compared to CIS, but it is still large for acetone, see Table 3. In contrast, the DFT methods underestimate the oscillator strengths. The only exceptions are LC-BLYP for all of the molecules and LC-ωPBE for acetaldehyde, as shown in Table 3 and Figure 1. This underestimation is particularly severe for acetone in many

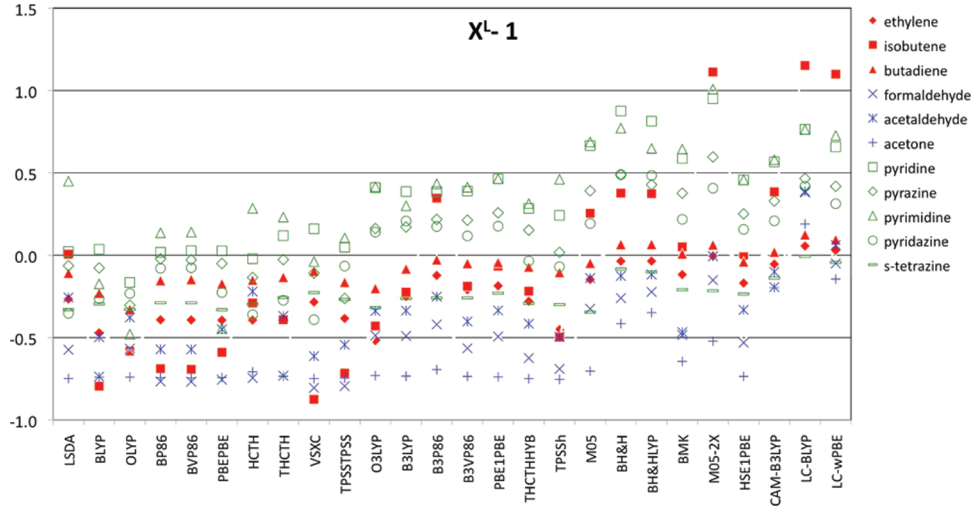

Figure 1. $X^L - 1$ for the single molecules.

cases. Very good performance is provided by LC-ωPBE and CAM-B3LYP, followed by BH&H and BH&HLYP. The R^2 values are much more scattered for this group, as shown in Figure 3. A general good behavior is reported for acetaldehyde, whereas poor results are obtained for formaldehyde and especially acetone with most of the pure and hybrid functionals with a small percentage of HF exchange (see Figure 3). CAM-B3LYP and LC-ωPBE provide a very good performance also for R^2, followed by BH&H and BH&HLYP. The X^L and R^2 values for the entire set (see Figures 2 and 4)

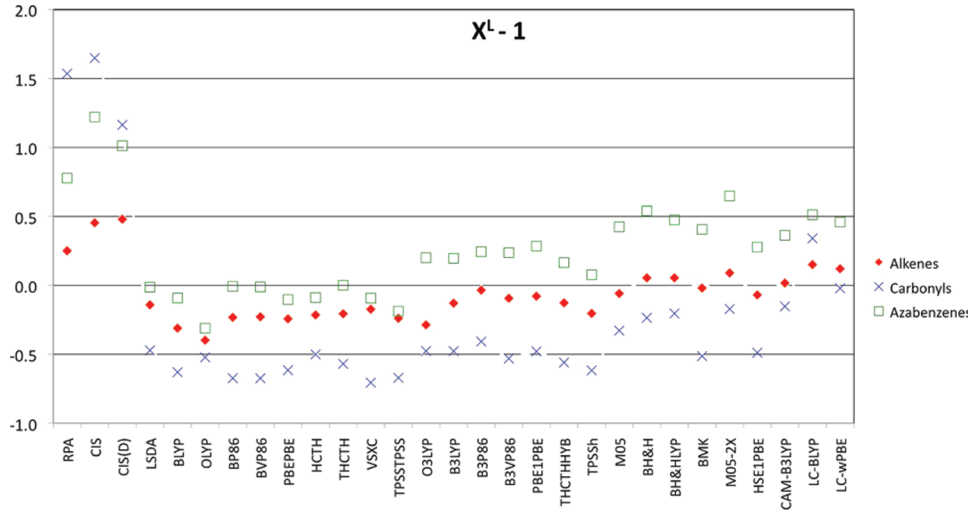

Figure 2. $X^L - 1$ for the molecular groups.

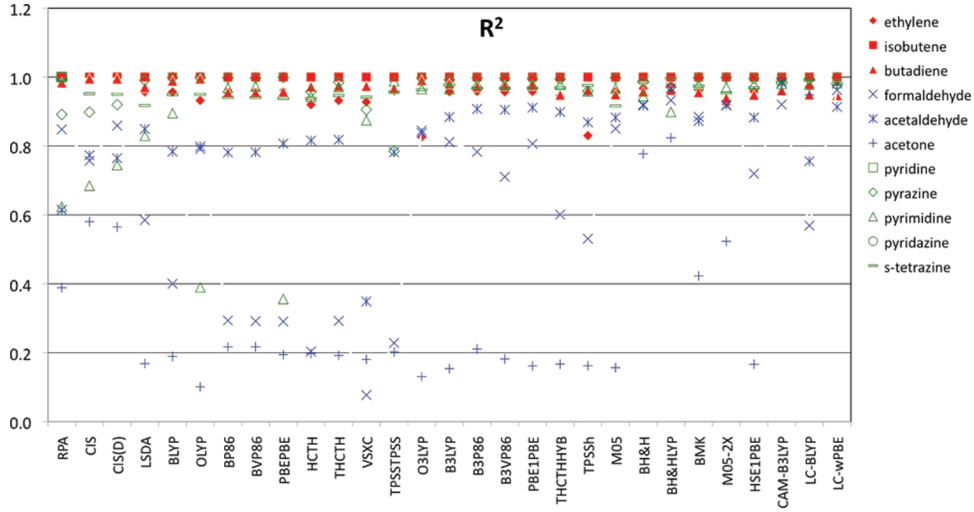

Figure 3. R^2 for the single molecules.

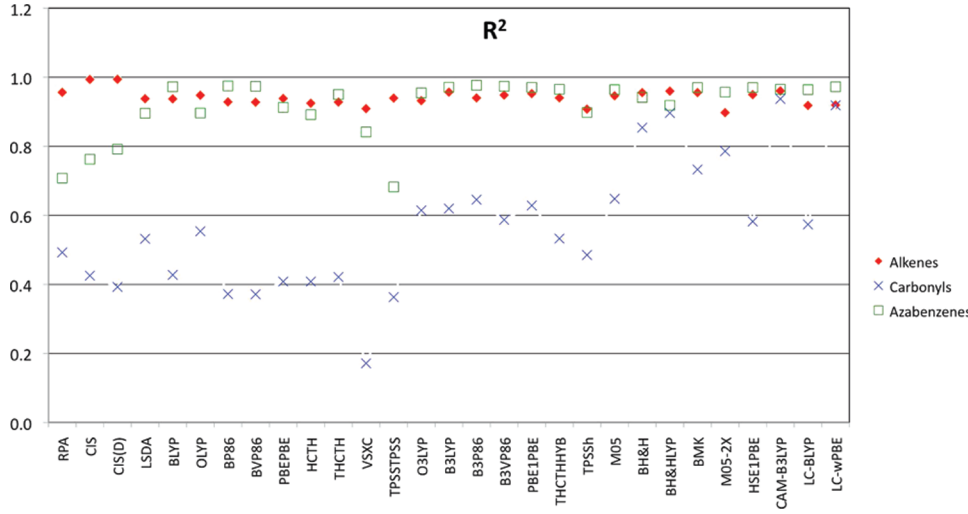

Figure 4. R^2 for the molecular groups.

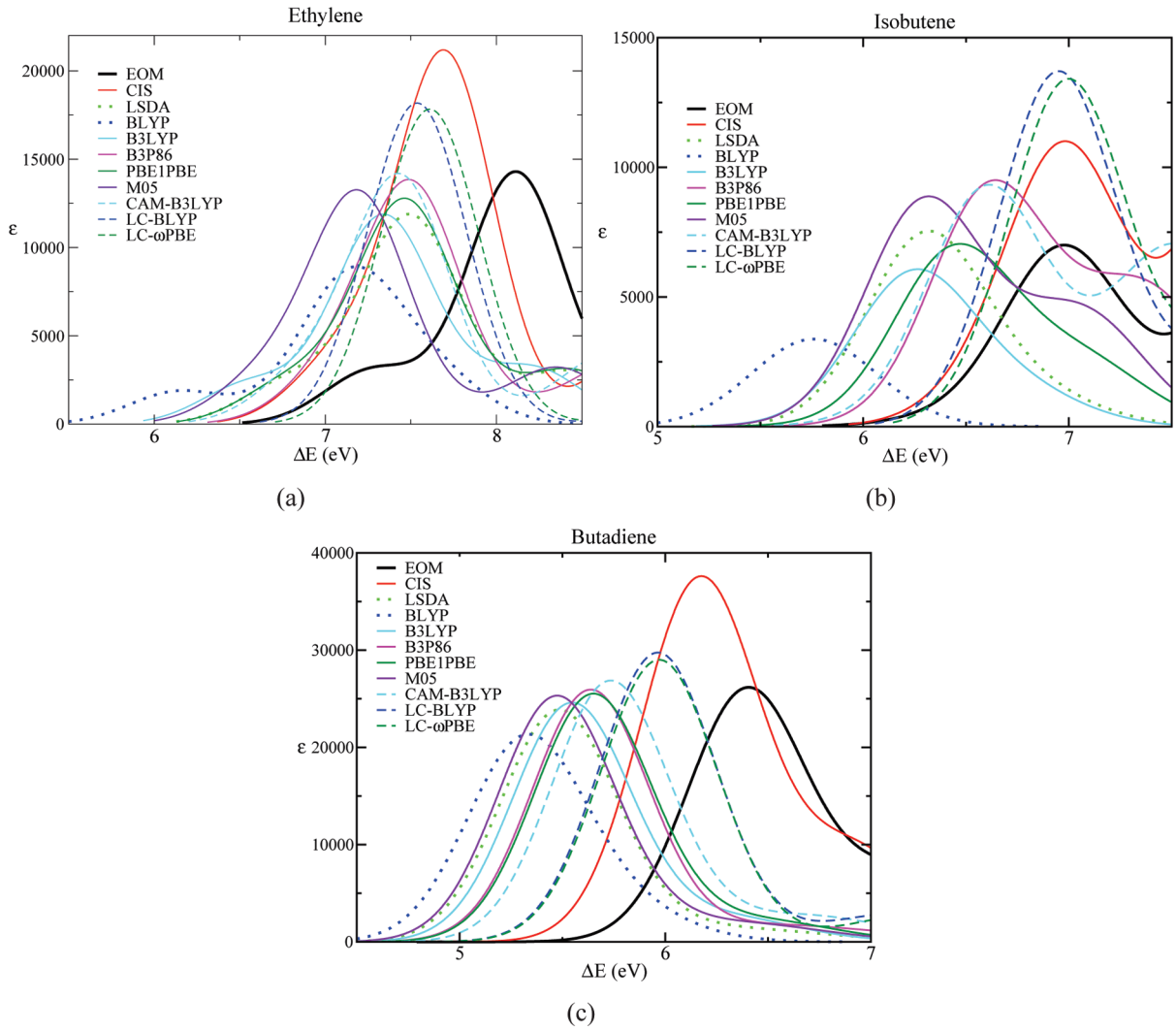

Figure 5. Alkenes spectra.

show a better performance moving from pure to hybrid functionals, especially those with large amounts of HF exchange. BH&H, BH&HLYP, CAM-B3LYP, and LC-ωPBE provide the overall best performance for this group.

In the azabenzene set, four transitions are considered for pyridine, five for pyrazine, six for pyrimidine, five for pyridazine, and four for s-tetrazine. The largest oscillator strengths are on the order of 8×10^{-2}. The X^L values are often larger than 2 for the WF methods, although RPA and CIS(D) provide rather good results for s-tetrazine (see Table 4). For the functionals, the magnitude of X^L seems to increase moving from left to right in Figure 1, i.e., going from pure functionals to hybrids with an increasing amount of HF exchange to functionals with short- and long-range separation. In this case, many pure functionals perform rather well, as do most of the hybrids with a small amount of HF exchange. CAM-B3LYP is the best among the long-range separated functionals. The R^2 values are reasonably good for almost all of the functionals with the exception of pyrimidine with OLYP and PBEPBE. The WF methods also show some difficulty with this molecule. The collective X^L results in Figure 2 show good performance of the pure functionals; this degrades for hybrid functionals, especially for those with a larger amount of HF exchange and short−long-range separation. On the other hand, the collective R^2 values in Figure 4 are very close to unity for most of the functionals.

4. Simulated Spectra

The spectrum of ethylene, Figure 5a, shows that all of the methods are shifted to lower energy compared to EOM-CCSD. CIS, LC-BLYP, and LC-ωPBE overestimate the intensity of the most intense band while the others are very close to the reference (only BLYP significantly underestimates it). Most of the DFT bands are centered around the same energy, while M05 and BLYP are shifted to lower energy. The small band centered at 7.3 eV for EOM-CCSD is not well reproduced by many methods, i.e., CIS, B3P86, M05, CAM-B3LYP, LC-BLYP, and LC-ωPBE. For these methods, the two bands are so close in energy that the large band covers the small one. For isobutene, Figure 5b, the CIS band is centered at the same energy of EOM-CCSD, but it is much more intense. The intensity of the band for LSDA, B3LYP, and PBE1PBE is similar to that for EOM-CCSD but shifted to lower energy. B3P86, M05, and CAM-B3LYP overestimate the intensity of the band, which is also shifted to lower energy. BLYP provides the worst performance with

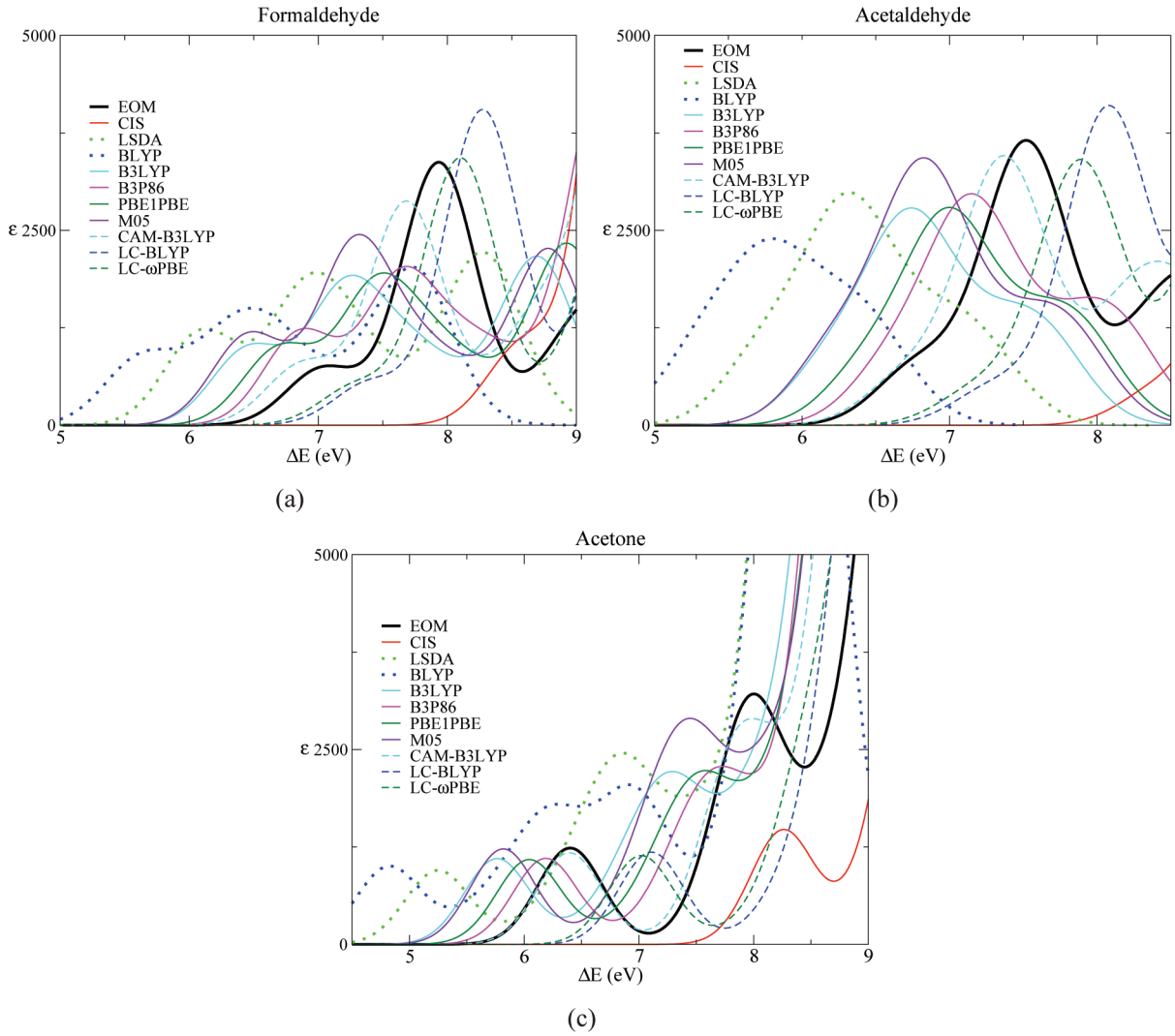

Figure 6. Carbonyls spectra.

a very small band at very low energy. LC-BLYP and LC-ωPBE have the band at the right energy, but the overestimation of its intensity is even greater than that for CIS. The butadiene spectrum, Figure 5c, is quite well reproduced by almost all of the functionals as far as the intensity of the band is concerned (the worst performance is again provided by BLYP), but the position of the bands is shifted to lower energy. The long-range corrected functionals overestimate the intensity of the band also in this case. CIS has the closest band to EOM-CCSD in terms of energy, but it is also the method that most overestimates the intensity.

The EOM-CCSD spectrum of formaldehyde has two bands at 7 and 8 eV (see Figure 6a). LSDA, BLYP, B3LYP, PBE1PBE, and M05 provide poor performance in this case, with bands of small intensity and shifted to lower energy. Poor performance is shown by CIS with very intense bands that are high in energy. CAM-B3LYP, LC-BLYP, and LC-ωPBE, on the other hand, satisfactorily reproduce the EOM-CCSD spectrum. CAM-B3LYP slightly underestimates the intensity of the band at 8 eV, while LC-BLYP and LC-ωPBE slightly overestimate it. B3P86 underestimates the intensity of the 8 eV band (similar to B3LYP and PBE1PBE), but its position is at the same energy as CAM-B3LYP. The spectrum of acetaldehyde, Figure 6b, is extremely overestimated by CIS both in the position and in the intensity of the bands (which are out of the energy range of the figure). The DFT methods do a better job with respect to the intensity, although only B3P86, CAM-B3LYP, and LC-ωPBE are close in energy to EOM-CCSD. The best agreement is provided by CAM-B3LYP with a spectrum slightly shifted to lower energy. For acetone, Figure 6c, CIS shows the usual large overestimation of the intensity and shifts to much higher energy. The opposite behavior is shown by LSDA and BLYP. The LC-BLYP and LC-ωPBE spectra are shifted to higher energy; these methods also miss the EOM-CCSD band at 8 eV. B3LYP, B3P86, and PBE1PBE similarly underestimate the intensity and position of the bands. Among these functionals, B3P86 is the closest to EOM-CCSD in terms of the energy. M05 provides a good performance for the intensity, but the bands are shifted to lower energy. The functional that best approximates the EOM-CCSD spectrum for this molecule in this energy range is CAM-B3LYP.

The azabenzenes have a small band at 5−5.5 eV and an intense band at 7.5−8 eV. For pyridine, Figure 7a, CIS overestimates the intensity of both, and their position is shifted to higher energy. All of the functionals simulate the EOM-CCSD spectrum more closely, although the intense

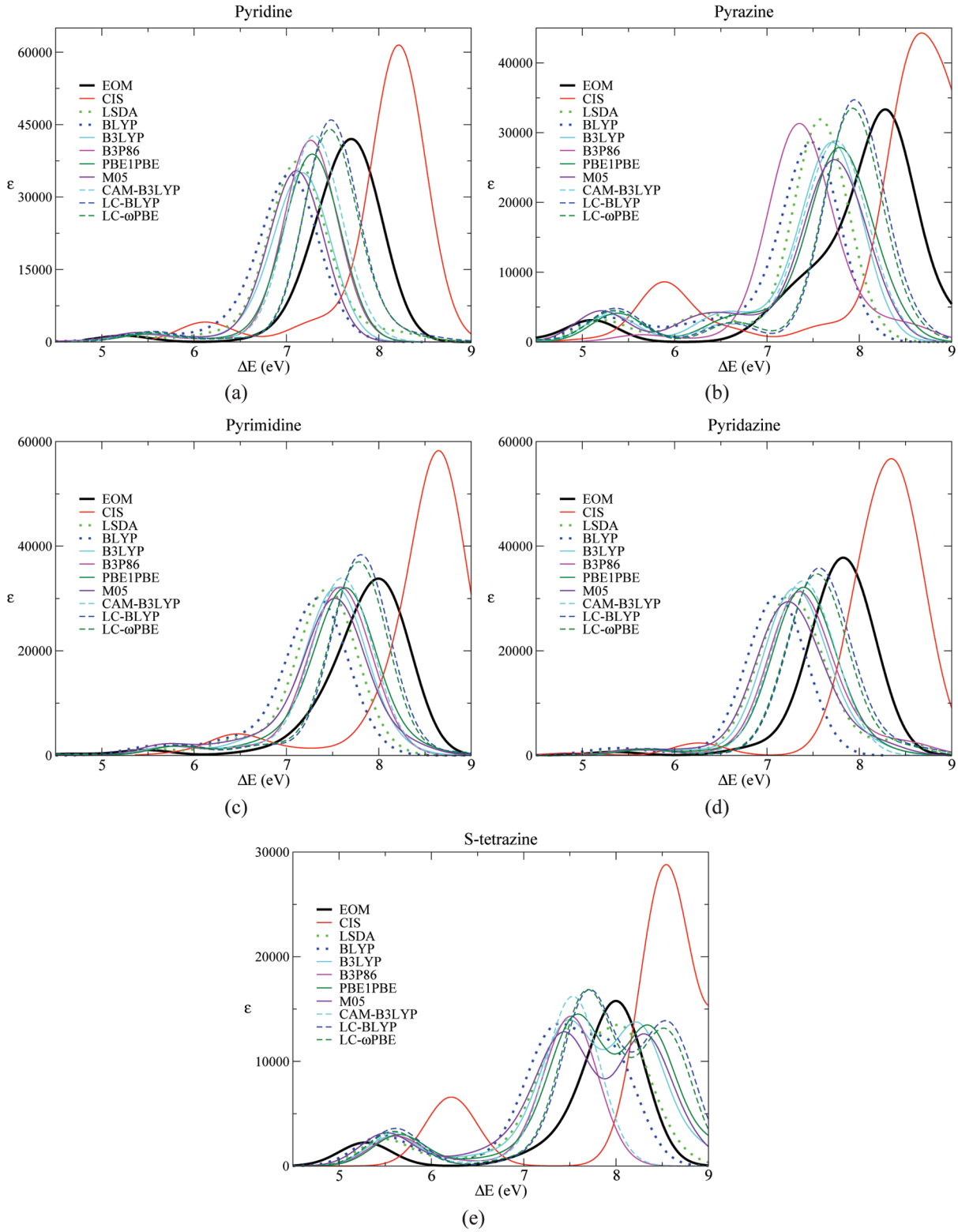

Figure 7. Azabenzenes spectra.

band is shifted to lower energy. For pyrazine, Figure 7b, the small band around 5 eV is shifted to higher energy with all of the methods. On the other hand, the more intense band is shifted to lower energy with all of the functionals (the CIS band is at higher energy). The best agreement with EOM-CCSD is obtained with LC-BLYP and LC-ωPBE, both in the intensity and in the position of the band. The other functionals underestimate the intensity of this band, although the intensities of the B3P86 and LSDA bands are close to that of EOM-CCSD. For pyrimidine, Figure 7c, similar considerations apply. However, in this case, the difference in the intensity of the large band is very small for most functionals. Only LC-BLYP and LC-ωPBE slightly overestimate the intensity of the EOM-CCSD band. CIS overestimates both bands in position and intensity. Pyridazine, Figure 7d, has a spectrum very similar to that of pyrimidine.

All of the methods behave comparably to the previous molecule, though the intensity of the large EOM-CCSD band is slightly underestimated by all of the functionals. Finally, s-tetrazine has a spectrum less intense in the same region (Figure 7e). LC-BLYP and LC-ωPBE reproduce the EOM-CCSD spectrum rather well, though the position of the small band is at higher energy while that of the larger band is at lower energy. The intensity of the large CAM-B3LYP band is comparable to that of EOM-CCSD, but it is centered at a slightly lower energy than those of LC-BLYP and LC-ωPBE. The third band shown by many functionals is outside the energy range considered for EOM-CCSD. Note that, with the exception of B3P86, CAM-B3LYP, LC-BLYP, and LC-ωPBE, the DFT methods require a large number of states to completely characterize the intense band for this set of molecules: around 30−40 states for the hybrid functionals and around 60−80 states for LSDA and BLYP.

5. Discussion and Conclusion

The results in sections 3 and 4 show that more approximate WF methods such as RPA, CIS, and CIS(D) consistently overestimate the oscillator strength compared to EOM-CCSD, as they do for the excitation energy. Additionally, the R^2 values show that the oscillator strengths are quite scattered compared to EOM-CCSD for the carbonyls and part of the azabenzenes. However, the CIS plots in section 4 qualitatively reproduce the EOM-CCSD spectra.

On the contrary, pure functionals mostly underestimate the oscillator strength (and the excitation energy[12]), in many cases dramatically, as is evident in Figure 1. Some good results are obtained for azabenzenes. The R^2 values in Figures 3 and 4 show good alignment for alkenes and azabenzenes but not for the carbonyls. The performance of LSDA and BLYP on the simulated spectra in section 4, where many states had to be included to completely characterize the most intense bands of the azabenzenes, suggests that several low lying Rydberg states appear. The underestimation of excitations to Rydberg states is a well-known problem of pure functionals,[41,66,83,84] which makes these functionals computationally expensive since many states need to be sought in order to include the ones of interest.

Hybrid functionals with a small percentage of HF exchange and no short−long-range separation tend to underestimate the oscillator strength for alkenes and carbonyls and overestimate it for azabenzenes. For these functionals, the R^2 values are close to unity for alkenes and azabenzenes but not for the carbonyl compounds, in particular, acetone. A larger amount of HF exchange shifts X^L (both individual and collective) to higher values, such that $X^L \simeq 1$ for the alkenes, $X^L < 1$ for the carbonyls, and $X^L > 1$ for the azabenzenes (see Figures 1 and 2). The R^2 parameters are closer to unity than for the pure functionals, but they are still rather small for the carbonyls, especially acetone. For the latter, a larger amount of HF exchange provides better results. The carbonyl set represents a difficult test for these functionals (and even more for pure functionals) since all of the relevant excitations considered in section 3 are to Rydberg states, whereas for the azabenzenes, all of the states are valence, and for the alkenes the very bright valence states are predominant. In the simulated spectra in section 4, we noticed a mixing of valence and Rydberg states, which leads to a redistribution of the intensity among several transitions as previously reported by Tozer et al.[10] However, this is hidden in the simulated spectra due to summing of the Gaussian line shapes. The simulated spectra in section 4 usually show less intense bands than EOM-CCSD with all of the functionals that do not separate short- and long-range effects. B3P86 stands out among these functionals as an excellent choice.

Three of the short−long-range separated functionals (CAM-B3LYP, LC-BLYP, and LC-ωPBE) perform on average better than the other functionals in reproducing the EOM-CCSD results, especially for difficult cases like acetone. This is shown in both the statistical analysis and the simulated spectra. In particular, CAM-B3LYP is often very close to the reference results, although it does not have the correct asymptotic behavior in the long range. LC-ωPBE also behaves well despite some difficulty with some azabenzenes and the significant overestimation of the isobutene oscillator strength for the bright A_1 state. CAM-B3LYP and LC-ωPBE also show the R^2 value closest to 1. In the simulated spectra, the two functionals with the correct asymptotic behavior, LC-BLYP and LC-ωPBE, often show more intense bands than EOM-CCSD.

For the data set we analyzed, i.e., Rydberg and valence states for small organic molecules, the magnitude of X^L increases moving from pure functionals to hybrids with more and more HF exchange. On the other hand, the WF methods in this work largely overestimate EOM-CCSD. More importantly, the results in Figures 1 and 2 seem to indicate that it is not possible to define a single scaling factor for the oscillator strength computed with the approximate functionals. In fact, $0.5 < X^L < 1.5$ depending on the set of molecules. On average, the best performance for the test cases considered here is obtained with CAM-B3LYP in both the statistical analysis and the simulation of the spectra, followed by LC-ωPBE. LC-BLYP also shows quite good agreement with EOM-CCSD. Among the functionals with no short−long-range separation, B3P86 provides satisfactory results with spectra often very close to those of CAM-B3LYP. As outlined in ref 12, the range of functionals and test cases considered in this work is certainly not complete. Nevertheless, these results provide useful insight on the ability of many current functionals to produce oscillator strengths of EOM-CCSD quality and show how much work is still necessary in the development of density functional theory.

Acknowledgment. M.C. thanks Prof. H. Bernhard Schlegel for encouraging this research and for stimulating discussions and Dr. Richard L. Lord for carefully reading the manuscript.

Supporting Information Available: Values of the oscillator strength and R^2 for all of the methods and the states in section 3. Extra diffuse functions added to the standard 6-311++G(d,p) basis to form the 6-311(3+,3+)G(d,p) basis set used in this work and in ref 12. This material is available free of charge via the Internet at http://pubs.acs.org.

References

(1) Casida, M. E. *Recent Advances in Density Functional Methods*; World Scientific: Singapore, 1995; Vol. 1.

(2) Casida, M. E. *Recent Developments and Applications of Modern Density Functional Theory, Theoretical and Computational Chemistry*; Elsevier: Amsterdam, 1996; Vol. 4.

(3) Stratmann, R. E.; Scuseria, G. E.; Frisch, M. J. *J. Chem. Phys.* **1998**, *109*, 8218–8224.

(4) Wiberg, K. B.; de Oliveira, A. E.; Trucks, G. *J. Phys. Chem. A* **2002**, *106*, 4192–4199.

(5) Sousa, S. F.; Fernandes, P. A.; Ramos, M. J. *J. Phys. Chem. A* **2007**, *111*, 10439–10452.

(6) Zhang, G.; Musgrave, C. B. *J. Phys. Chem. A* **2007**, *111*, 1554–1561.

(7) Silva-Junior, M. R.; Schreiber, M.; Sauer, S. P. A.; Thiel, W. *J. Chem. Phys.* **2008**, *129*, 104103.

(8) Silva-Junior, M. R.; Sauer, S. P. A.; Schreiber, M.; Thiel, W. *Mol. Phys.* **2010**, *108*, 453–465.

(9) Silva-Junior, M. R.; Schreiber, M.; Sauer, S. P. A.; Thiel, W. *J. Chem. Phys.* **2010**, *133*, 174318.

(10) Tozer, D. J.; Amos, R. D.; Handy, N. C.; Roos, B. O.; Serrano-Andrés, L. *Mol. Phys.* **1999**, *97*, 859–868.

(11) Jacquemin, D.; Wathelet, V.; Perpète, E. A.; Adamo, C. *J. Chem. Theory Comput.* **2009**, *5*, 2420–2435, and references therein.

(12) Caricato, M.; Trucks, G. W.; Frisch, M. J.; Wiberg, K. B. *J. Chem. Theory Comput.* **2010**, *6*, 370–383.

(13) Jacquemin, D. V.; Perpète, E. A.; Ciofini, I.; Adamo, C. *Theor. Chem. Acc.* **2010**, *1*, 10 .

(14) Plötner, J.; Tozer, D. J.; Dreuw, A. *J. Chem. Theory Comput.* **2010**, *6*, 2315–2324.

(15) Jacquemin, D. V.; Perpete, E. A.; Ciofini, I.; Adamo, C.; Valero, R.; Zhao, Y.; Truhlar, D. G. *J. Chem. Theory Comput.* **2010**, *6*, 2071–2085.

(16) Jacquemin, D. V.; Perpète, E. A.; Ciofini, I.; Adamo, C. *J. Chem. Theory Comput.* **2010**, *6*, 1532–1537.

(17) Wiberg, K. B.; Hadad, C. M.; Ellison, G. B.; Foresman, J. B. *J. Phys. Chem.* **1993**, *97*, 13586–13597.

(18) Hadad, C. M.; Foresman, J. B.; Wiberg, K. B. *J. Phys. Chem.* **1993**, *97*, 4293–4312.

(19) Bolovinos, A.; Tsekeris, P.; Philis, J.; Pantos, E.; Andritsopoulos, G. *J. Mol. Spectrosc.* **1984**, *103*, 240–256.

(20) Walker, I. C.; Palmer, M. H.; Hopkirk, A. *Chem. Phys.* **1990**, *141*, 365–378.

(21) Goodman, L. *J. Mol. Spectrosc.* **1961**, *6*, 109–137.

(22) Innes, K. K.; Ross, I. G.; Moomaw, W. R. *J. Mol. Spectrosc.* **1988**, *132*, 492–544.

(23) Palmer, M. H.; Walker, I. C. *Chem. Phys.* **1991**, *157*, 187–200.

(24) Palmer, M. H.; McNab, H.; Reed, D.; Pollacchi, A.; Walker, I. C.; Guest, M. F.; Siggel, M. R. F. *Chem. Phys.* **1997**, *214*, 191–211.

(25) Spencer, G. H.; Cross, P. C.; Wiberg, K. B. *J. Chem. Phys.* **1961**, *35*, 1925–1938.

(26) Adamo, C.; Barone, V. *Chem. Phys. Lett.* **2000**, *330*, 152–160.

(27) Nooijen, M. *J. Phys. Chem. A* **2000**, *104*, 4553–4561.

(28) Devarajan, A.; Gaenko, A. V.; Khait, Y. G.; Hoffmann, M. R. *J. Phys. Chem. A* **2008**, *112*, 2677–2682.

(29) For ethylene, we inverted the order of the two $1B_{1u}$ states in our previous work[12] for the following functionals: BLYP, OLYP, BP86, BVP86, PBEPBE, HCTH, THCTH, VSXC, TPSSTPSS, and TPSSh. Since the excitation energies for these two states are close to each other with these functionals, their final performance for this molecule is unchanged.

(30) Foresman, J. B.; Head-Gordon, M.; Pople, J. A.; Frisch, M. J. *J. Phys. Chem.* **1992**, *96*, 135–149.

(31) Head-Gordon, M.; Rico, R. J.; Oumi, M.; Lee, T. J. *Chem. Phys. Lett.* **1994**, *219*, 21–29.

(32) McWeeny, R. *Methods of Molecular Quantum Mechanics*, 2nd ed.; Academic Press: London, 1992.

(33) Bartlett, R. J.; Musial, M. *Rev. Mod. Phys.* **2007**, *79*, 291–352.

(34) Sekino, H.; Bartlett, R. J. *Int. J. Quantum Chem.: Quantum Chem. Symp.* **1984**, *18*, 255–265.

(35) Stanton, J. F.; Bartlett, R. J. *J. Chem. Phys.* **1993**, *98*, 7029–7039.

(36) Miura, M.; Aoki, Y.; Champagne, B. *J. Chem. Phys.* **2007**, *127*, 084103.

(37) Jacquemin, D.; Perpete, E. A. *THEOCHEM* **2007**, *804*, 31–34.

(38) Hirata, S.; Lee, T. J.; Head-Gordon, M. *J. Chem. Phys.* **1999**, *111*, 8904–8912.

(39) Tokura, S.; Tsuneda, T.; Hirao, K. *J. Theory Comput. Chem.* **2006**, *5*, 925–944.

(40) Matsuzawa, N. N.; Ishitani, A.; Dixon, D. A.; Uda, T. *J. Phys. Chem. A* **2001**, *105*, 4953–4962.

(41) Casida, M. E.; Salahub, D. R. *J. Chem. Phys.* **2000**, *113*, 8918–8935.

(42) Guillaumont, D.; Nakamura, S. *Dyes Pigment.* **2000**, *46*, 85–92.

(43) Peach, M. J. G.; Le Sueur, C. R.; Ruud, K.; Guillaumeb, M.; Tozer, D. J. *Phys. Chem. Chem. Phys.* **2009**, *11*, 4465–4470.

(44) Slater, J. C. *Phys. Rev.* **1951**, *81*, 385–390.

(45) Becke, A. D. *Phys. Rev. A* **1988**, *38*, 3098–3100.

(46) Lee, C. T.; Yang, W. T.; Parr, R. G. *Phys. Rev. B* **1988**, *37*, 785–789.

(47) Becke, A. D. *J. Chem. Phys.* **1993**, *98*, 5648–5652.

(48) Vosko, S. H.; Wilk, L.; Nusair, M. *Can. J. Phys.* **1980**, *58*, 1200–1211.

(49) Handy, N. C.; Cohen, A. J. *Mol. Phys.* **2001**, *99*, 403–412.

(50) Perdew, J. P. *Phys. Rev. B* **1986**, *33*, 8822–8824.

(51) Hamprecht, F. A.; Cohen, A. J.; Tozer, D. J.; Handy, N. C. *J. Chem. Phys.* **1998**, *109*, 6264–6271.

(52) Van Voorhis, T.; Scuseria, G. E. *J. Chem. Phys.* **1998**, *109*, 400–410.

(53) Perdew, J. P.; Burke, K.; Ernzerhof, M. *Phys. Rev. Lett.* **1996**, *77*, 3865–3868.

(54) Perdew, J. P.; Burke, K.; Ernzerhof, M. *Phys. Rev. Lett.* **1997**, *78*, 1396–1396.

(55) Boese, A.; Doltsinis, N.; Handy, N.; Sprik, M. *J. Chem. Phys.* **2000**, *112*, 1670–1678.

(56) Boese, A. D.; Handy, N. C. *J. Chem. Phys.* **2001**, *114*, 5497–5503.

(57) Boese, A. D.; Handy, N. C. *J. Chem. Phys.* **2002**, *116*, 9559–9569.

(58) Hoe, W. M.; Cohen, A. J.; Handy, N. C. *Chem. Phys. Lett.* **2001**, *341*, 319–328.

(59) Tao, J. M.; Perdew, J. P.; Staroverov, V. N.; Scuseria, G. E. *Phys. Rev. Lett.* **2003**, *91*, 146401.

(60) Zhao, Y.; Schultz, N. E.; Truhlar, D. G. *J. Chem. Phys.* **2005**, *123*, 161103.

(61) Zhao, Y.; Schultz, N. E.; Truhlar, D. G. *J. Chem. Theory Comput.* **2006**, *2*, 364–382.

(62) Boese, A. D.; Martin, J. M. L. *J. Chem. Phys.* **2004**, *121*, 3405–3416.

(63) Heyd, J.; Scuseria, G. E.; Ernzerhof, M. *J. Chem. Phys.* **2003**, *118*, 8207–8215.

(64) Yanai, T.; Tew, D. P.; Handy, N. C. *Chem. Phys. Lett.* **2004**, *393*, 51–57.

(65) Iikura, H.; Tsuneda, T.; Yanai, T.; Hirao, K. *J. Chem. Phys.* **2001**, *115*, 3540–3544.

(66) Tawada, T.; Tsuneda, T.; Yanagisawa, S.; Yanai, T.; Hirao, K. *J. Chem. Phys.* **2004**, *120*, 8425–8433.

(67) Vydrov, O. A.; Scuseria, G. E. *J. Chem. Phys.* **2006**, *125*, 234109.

(68) Vydrov, O. A.; Heyd, J.; Krukau, V.; Scuseria, G. E. *J. Chem. Phys.* **2006**, *125*, 074106.

(69) Adamo, C.; Barone, V. *J. Chem. Phys.* **1999**, *110*, 6158–6170.

(70) Ernzerhof, M.; Scuseria, G. E. *J. Chem. Phys.* **1999**, *110*, 5029–5036.

(71) Stephens, P. J.; Devlin, F. J.; Ashvar, C. S.; Chabalowski, C. F.; Frisch, M. J. *Faraday Discuss.* **1994**, *99*, 103–119.

(72) Stephens, P. J.; Devlin, F. J.; Chabalowski, C. F.; Frisch, M. J. *J. Chem. Phys.* **1994**, *98*, 11623–11627.

(73) Staroverov, V. N.; Scuseria, G. E.; Tao, J. M.; Perdew, J. P. *J. Chem. Phys.* **2003**, *119*, 12129–12137.

(74) Becke, A. D. *J. Chem. Phys.* **1993**, *98*, 1372–1377.

(75) Frisch, M. J.; Trucks, G. W.; Schlegel, H. B.; Scuseria, G. E.; Robb, M. A.; Cheeseman, J. R.; Montgomery, J. A., Jr.; Vreven, T.; Scalmani, G.; Mennucci, B.; Barone, V.; Petersson, G. A.; Caricato, M.; Nakatsuji, H.; Hada, M.; Ehara, M.; Toyota, K.; Fukuda, R.; Hasegawa, J.; Ishida, M.; Nakajima, T.; Honda, Y.; Kitao, O.; Nakai, H.; Li, X.; Hratchian, H. P.; Peralta, J. E.; Izmaylov, A. F.; Kudin, K. N.; Heyd, J. J.; Brothers, E.; Staroverov, V. N.; Zheng, G.; Kobayashi, R.; Normand, J.; Sonnenberg, J. L.; Ogliaro, F.; Bearpark, M.; Parandekar, P. V.; Ferguson, G. A.; Mayhall, N. J.; Iyengar, S. S.; Tomasi, J.; Cossi, M.; Rega, N.; Burant, J. C.; Millam, J. M.; Klene, M.; Knox, J. E.; Cross, J. B.; Bakken, V.; Adamo, C.; Jaramillo, J.; Gomperts, R.; Stratmann, R. E.; Yazyev, O.; Austin, A. J.; Cammi, R.; Pomelli, C.; Ochterski, J. W.; Ayala, P. Y.; Morokuma, K.; Voth, G. A.; Salvador, P.; Dannenberg, J. J.; Zakrzewski, V. G.; Dapprich, S.; Daniels, A. D.; Strain, M. C.; Farkas, O.; Malick, D. K.; Rabuck, A. D.; Raghavachari, K.; Foresman, J. B.; Ortiz, J. V.; Cui, Q.; Baboul, A. G.; Clifford, S.; Cioslowski, J.; Stefanov, B. B.; Liu, G.; Liashenko, A.; Piskorz, P.; Komaromi, I.; Martin, R. L.; Fox, D. J.; Keith, T.; Al-Laham, M. A.; Peng, C. Y.; Nanayakkara, A.; Challacombe, M.; Chen, W.; Wong, M. W.; Pople, J. A. *Gaussian Development Version*, Revision G.01+; Gaussian, Inc.: Wallingford, CT, 2008.

(76) Del Bene, J. E.; Watts, J. D.; Bartlett, R. J. *J. Chem. Phys.* **1997**, *106*, 6051–6060.

(77) Stanton, J. F.; Gauss, J.; Ishikawa, N.; Head-Gordon, M. *J. Chem. Phys.* **1995**, *103*, 4160–4174.

(78) Koch, H.; Jorgensen, P. *J. Chem. Phys.* **1990**, *93*, 3333–3344.

(79) Kallay, M.; Gauss, J. *J. Chem. Phys.* **2004**, *121*, 9257–9269.

(80) Koch, H.; Kobayashi, R.; Demeras, A. S.; Jorgensen, P. *J. Chem. Phys.* **1994**, *100*, 4393–4400.

(81) Caricato, M.; Trucks, G. W.; Frisch, M. J. *J. Chem. Phys.* **2009**, *131*, 174104.

(82) Harada, N.; Chen, S. L.; Nakanishi, K. *J. Am. Chem. Soc.* **1975**, *97*, 5345–5352.

(83) Tozer, D. J.; Handy, N. C. *J. Chem. Phys.* **1998**, *109*, 10180–10189.

(84) Casida, M. E.; Casida, K. C.; Salahub, D. R. *Int. J. Quantum Chem.* **1998**, *70*, 933–941.

CT100662N